

Extraction of a 3D graph structure of wormholes in a wooden statue of Buddha by X-ray CT image analysis

Junko Iwamoto, Yukiko Kenmochi, Kazunori Kotani
 School of Information Science
 Japan Advanced Institute of Science and Technology
 1-1 Asahidai, Tatsunokuchi Ishikawa Japan
 {jiwamoto, kenmochi, ikko}@jaist.ac.jp

Ichiro Nagasawa
 Tokyo National University
 of Fine Arts and Music
 12-8 Ueno Kouen, Taito-ku, Tokyo Japan
 nagasawa@fa.geidai.ac.jp

Abstract

The high historical and precious wooden statues of Buddha, have received serious damages by cracking, corrosion, wormholes, etc., because of the quality of the materials of woods. For the restoration of such damaged statues, the advance inspections of their interior conditions without destroying them are demanded.

In this paper, we meet such a demand by taking the X-ray CT images and by applying some techniques of image analysis for extraction of image features which are useful for the restoration. Especially, we focus on wormhole regions which are the most serious damages. We first present a method of the region segmentation and then consider extraction of a 3D graph structure of wormhole regions. Since each node of the graph possesses the geometric information such as a location, and a diameter of each wormhole, we show that the graph structures are useful for visualizing wormholes.

1. Introduction

There are many high historical and precious wooden statues of Buddha which had been made several hundred years ago. It is also known that most of them have received serious damages due to the quality of the materials of woods by cracks, corrosion, wormholes, etc. Although the restoration work has been performed for remaining the precious cultural property to our future generations, it has not progressed sufficiently because much knowledge and the high-level skills are indispensable [1].

The wormholes are the most serious damages in wooden statues of Buddha. The problem is that the solidity becomes weak gradually when wormholes are evolving. Sometimes, a statue of Buddha loses its original form. For a countermeasure, sculptors of Buddhist statues diagnose the dam-

ages by using the X-ray photographs or the X-ray CT images. To recover statues of Buddha, they inject filler for reinforcement and repair. For more efficient diagnosis and restoration, engineering supports such as automatic image analysis are expected. In this paper, we present methods to analyze the X-ray CT images and to extract some useful information on the damages.

We first propose a segmentation method of wormhole regions by using the 3D figure fusion processings [2]. Next, we extract the 3D graph structure of wormhole regions. The 3D graph expresses the structure of wormholes shaped like tubes with diameters from 0.1 to 4[mm]. Since each node of the graph possesses the geometric information, such as a location, and diameter of each wormhole, we show that not only the topological information but also those geometric information of the graph structure is useful for visualizing wormholes.

2. Statue region segmentation

2.1. Observation on the X-ray CT wooden statue images

An X-ray CT image is expressed by CT values. Let μ_t and μ_{water} be a X-ray absorption coefficient of an object and the water, respectively. Then, the CT value is obtained by

$$CTvalue = \frac{\mu_t - \mu_{water}}{\mu_{water}} \times K \quad (1)$$

where K is the Hounsfield value, 1000. In the X-ray CT images of wooden statues of Buddha, we have to consider the X-ray absorption coefficients of air, woods, and metals such as μ_{air} , μ_{wood} , μ_{metal} , and they have the following relations:

$$\mu_{air} < \mu_{wood} < \mu_{water} < \mu_{metal}. \quad (2)$$

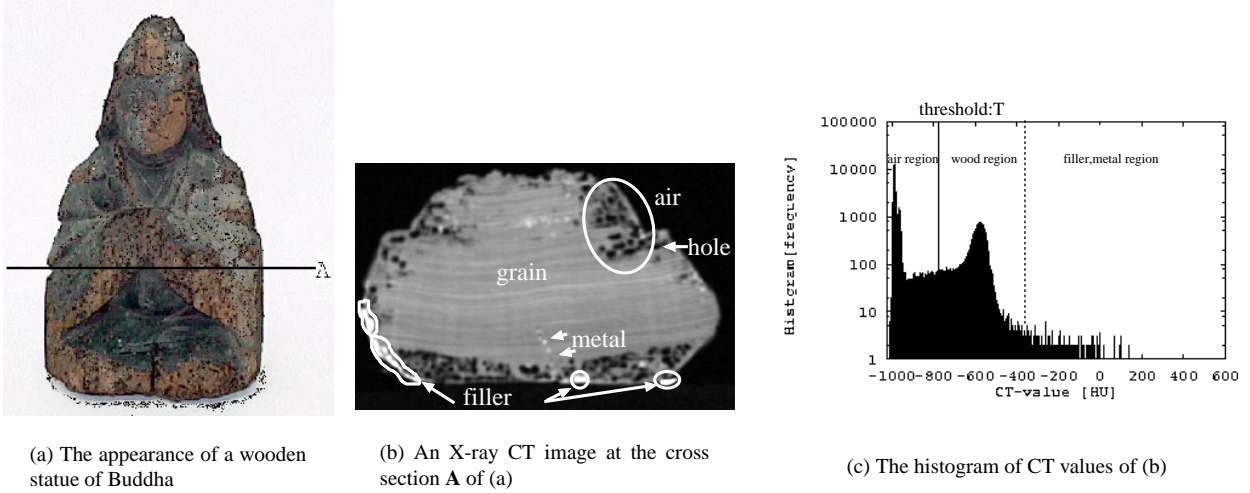


Figure 1. The appearance of a wooden statue of Buddha and a X-ray CT image

A cross-section image of a statue at the cross section A in Fig.1(a) is shown in Fig.1(b). It shows that there is a large difference between the CT value of a wood and that of a wormhole. The histogram of CT values of the cross-section image of Fig.1(b) is illustrated in Fig.1(c), and we see that there are two peaks. Because the peaks correspond to the different materials, we can separate air regions (a background and wormhole regions) from other regions (wood, filler and metal regions) by thresholding. However, the thresholding cannot divide the air region into the wormhole regions and the background. Thus, we first estimate the region of a statue of Buddha including wormhole regions, and then extract wormhole regions.

The outward form of a statue of Buddha is complex and rough. Therefore, it is difficult to extract such a complex contour of a statue of Buddha by using Snakes [3] which is useful for extracting a smooth surfaces. It is known that geometric object models are sometimes useful for object matching [4, 5]. However, it is difficult to find a specific geometric model in this case. In this paper, we therefore estimate the region of a statue of Buddha by using the 3D figure fusion processing [2].

2.2. Region Merging by figure fusion processing

Let Z^3 be a three-dimensional discrete space. Let us consider a 3D discrete image $F = \{f_{ijk}\}$, and each voxel $\mathbf{x} = (i, j, k) \in Z^3$ has the CT value f_{ijk} . The neighborhood of $\mathbf{x} \in Z^3$ is given by

$$\mathcal{N}_m(\mathbf{x}) = \left\{ \mathbf{y} \in Z^3 : \|\mathbf{x} - \mathbf{y}\| \leq \sqrt{t} \right\}, \quad (3)$$

and called the m -neighborhood for $m = 6, 18, 26$ where $t = 1, 2, 3$, respectively. Setting the erosion and dilation filter $\text{MAXF}[\mathcal{N}]$ and $\text{MINF}[\mathcal{N}]$ as follows:

$$\text{MINF}[\mathcal{N}] : \mathbf{F} = \{f_{ijk}\} \rightarrow \mathbf{G} = \{g_{ijk}\} \quad (4)$$

$$\text{where } g_{ijk} = \min \{f_{pqr} : (p, q, r) \in \mathcal{N}_m(i, j, k)\},$$

$$\text{MAXF}[\mathcal{N}] : \mathbf{F} = \{f_{ijk}\} \rightarrow \mathbf{G} = \{g_{ijk}\} \quad (5)$$

$$\text{where } g_{ijk} = \max \{f_{pqr} : (p, q, r) \in \mathcal{N}_m(i, j, k)\},$$

the 3D figure fusion operators are defined as their recursive filter such as,

$$\text{FU}_1[n, \mathcal{N}] = (\text{MAXF}[\mathcal{N}])^n \circ (\text{MINF}[\mathcal{N}])^n, \quad (6)$$

$$\text{FU}_2[n, \mathcal{N}] = (\text{MINF}[\mathcal{N}])^n \circ (\text{MAXF}[\mathcal{N}])^n. \quad (7)$$

In the reference [6], both FU_1 and FU_2 are used. How-

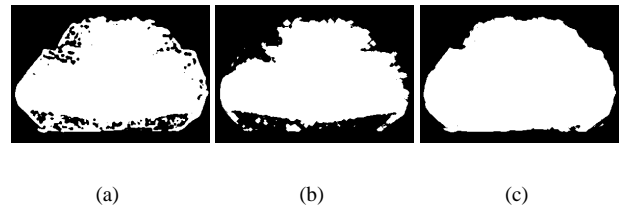


Figure 2. An initial image (a) and the image before and after the operations by FU_1 (b) and FU_2 (c)

ever, if we apply FU_1 for estimation of the region of a

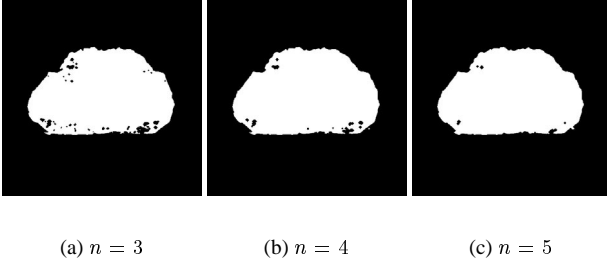


Figure 3. Images after the 3D figure fusion processing FU_2 of parameter n

statue of Buddha including wormholes, the interior wormhole regions will be expanded and the contour of a statue of Buddha will be changed as shown is Fig.2(b). Thus, we do not use FU_1 of (6) and estimate the region only by using FU_2 of (7) which proceeds erosion after dilation.

The parameters are determined by our preliminary experiment. We set $T = -780[HU]$ and $m = 6$ in eq. (2) (i.e. we choose the 6-neighborhood). The restoration work will be done for wormholes whose diameters are from 2 to $3[mm]$. Since the size of each pixel of the X-ray CT images used here is $0.4[mm/pixel]$, we set $n = 4$ (Fig.3(b)), in order to merge the statue region into wormhole regions whose diameters are about $3[mm]$ ¹. This is because the holes cannot fully unite when $n = 3$ (Fig.3(a)), and the outward form is expanded incorrectly when we set $n = 5$ (Fig.3(c)).

2.3. Algorithm for region estimation

We now give an algorithm for the region estimation of a statue of Buddha:

Algorithm 1

input: an X-ray CT image $\{f_{ijk}\}$.

output: a binary image $\{g_{ijk}\}$.

1. For each slice k , set the initial binary image $\{g_{ijk}\}$ by thresholding such that

$$g_{ijk} = \begin{cases} 1, & (f_{ijk} \geq T_k) \\ 0, & (f_{ijk} < T_k). \end{cases}$$

2. In each slice k , merge the wormhole regions into the wood regions by using a 3D figure fusion filter FU_2 of (7).
3. In each slice k , remove isolated wormhole regions, if the regions cannot be merged in **step 2**.

¹ $0.4[mm/pixel] \times 2 \times 4[pixel] = 3.2[mm]$

Obviously, the wormhole regions can be obtained from $\{f_{ijk}\}$ and $\{g_{ijk}\}$.

3. Graph structure extraction of wormhole regions

The useful information for the restoration of wooden statues damages by wormholes is, for example, the number, ramifications, locations, lengths and volumes of the branches of wormholes. In this paper, we thus describe the structure of wormholes by using a 3D graph whose nodes possess the geometric features above.

3.1. Features of wormhole structures

From the simple observation on the wormhole regions we see the following features:

1. A wormhole has the shape like a tube whose diameter is from 0.1 to $4[mm]$.
2. A wormhole may have several branches, with intersections, loops and ends, and there is no regular rule of the structures.

3.2. 3D graph structural extraction

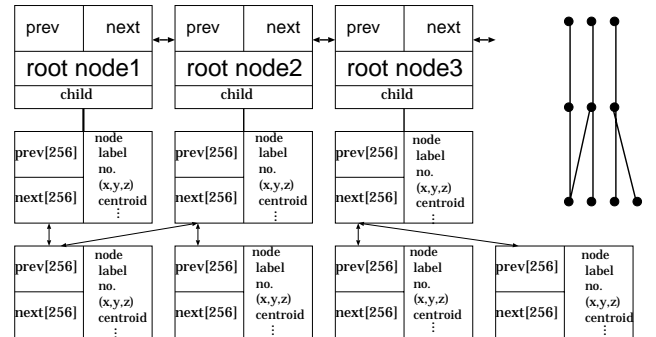


Figure 4. The data structure of a 3D graph for wormhole

In this paper, we consider that a wormhole region in each image slice corresponds to a node of a 3D graph, and a connectivity relations between wormholes regions of the two adjacent image slice corresponds to an edge. The list data structure of such a 3D graph illustrated in Fig.4 shows the case such that two or more branches (pre256, next256), and which has the information on nodes, such as the degree of circular and the algorithm of graph structure extraction as

follows:

Algorithm 2

input: an X-ray CT images $\{f_{ijk}\}$ and the binary image $\{g_{ijk}\}$ by **Algorithm 1**.

output: a graph with nodes $n_{k,l}$ and edges $e(n_{k,l}, n_{k+1,l'})$.

1. For each slice k ,
 - (a) Obtain a binary image

$$W_k = \{(i, j, k) \in Z^3 : w_{ijk} = 1\},$$

$$w_{ijk} = \begin{cases} 1, & \text{if } g_{ijk} = 1 \text{ and } f_{ijk} \leq T_k \\ 0, & \text{otherwise.} \end{cases}$$
 - (b) Divide W_k into the connected components $C_{k,l}$, $for l=1,2,3,\dots$ such that $\bigcup_{l=1,2,\dots} C_{k,l} = W_k$ and set the node $n_{k,l}$ for each $C_{k,l}$.
2. For each node $n_{k,l}$, calculate $out_{n_{k,l}}$ is more than a threshold. If consider the region $c_{k,l}$ as a part of the background rather than a wormhole region and remove $n_{k,l}$.

$$out_{n_{k,l}} = \frac{1}{|C_{k,l}|} \sum_{\substack{(p,q,r) \in C_{k,l} \\ (i,j,k) \in \mathcal{N}_m((i,j,k))}} (1 - g_{pqk}),$$

where $|C_{k,l}|$ is the number of elements in $C_{k,l}$.

3. For each $n_{k,l}$, if $C_{k,l}$ is connected to $C_{k+1,l'}$ make an edge $e(n_{k,l}, n_{k+1,l'})$.

3.3. Reconstruction of wormhole regions from a graph

Since each node $n_{k,l}$ keeps the corresponding wormhole region $C_{k,l}$, we can reconstruct all wormhole regions from $C_{k,l}$. A reconstructed image $R = \{r_{ijk}\}$ which is binary image is given by

$$r_{ijk} = \begin{cases} 1, & \text{if } (i, j, k) \in C_{k,l} \\ 0, & \text{otherwise.} \end{cases} \quad (8)$$

In addition, we can calculate other useful geometric features of wormhole regions such as the volume, diameters and centroids from these $C_{k,l}$. For visualization of a graph, we consider that each edge $e(n_{k,l}, n_{k+1,l'})$ is expressed by the line segment whose endpoints are the centroids of $C_{k,l}$ and $C_{k+1,l'}$.

4. Experiments

For our experiments, we prepared a set of synthetic images (32×32 [pixels], for each image). We used five of



(a) Synthetic images



(b) The estimation results of statue regions including wormholes



(c) The extraction results of wormhole regions by our method



(d) The extraction results of wormhole regions by thresholding

Figure 5. Test images and the experimental results of region estimation

the images as shown in Fig.5(a) for the wormhole region estimation and eight of them as shown in Fig.9(a) for an experiment of graph structure extraction is also don for X-ray CT images (512×512 [pixels], 173 [slices]) of a statue of Buddha in Fig.1(a).

4.1. Estimation of region from statue of Buddha

Table 1. Estimation errors of Fig.5(c)

	k [slice]				
	1	2	3	4	5
error ϵ_k [pixel]	0	0	0	1	2

For the synthetic images of Fig.5(a) we estimated the statue region including wormholes by applying **Algorithm 1**. The experimental results are shown in Fig.5(b). The

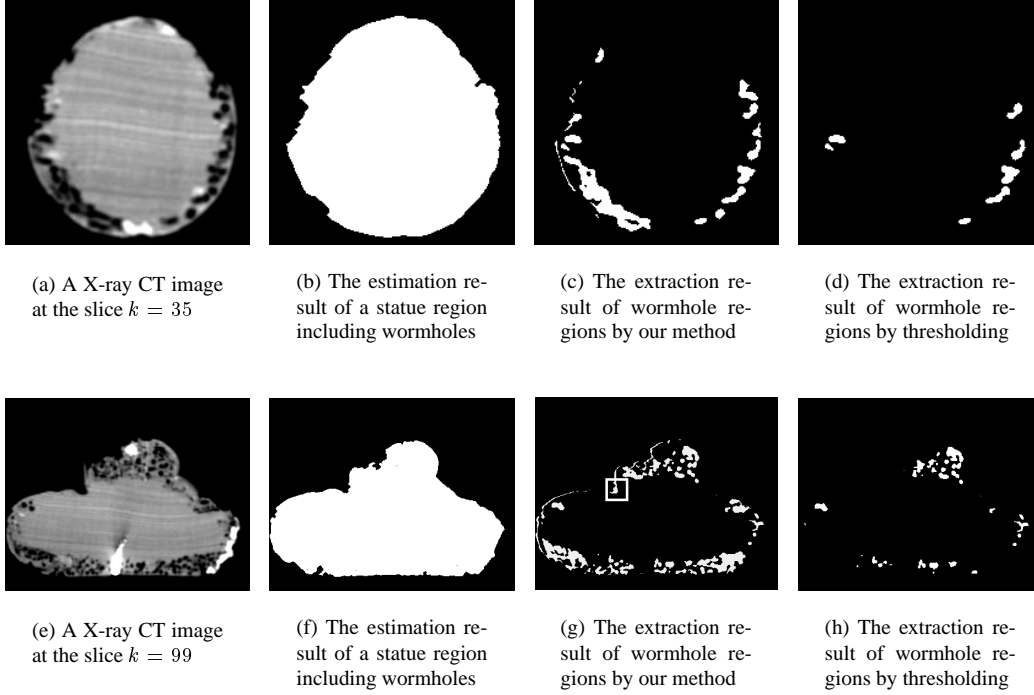


Figure 6. X-ray CT images and the experimental results of region estimation (slices of $k = 35, 99$)

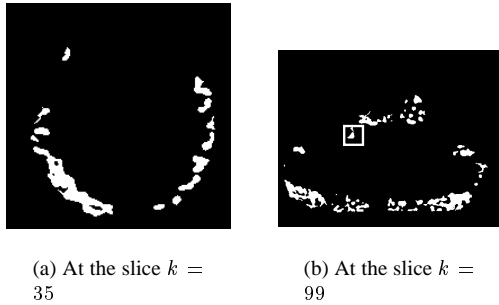


Figure 7. The extracted results by step2 of Algorithm 2

wormhole regions obtained by Eq.(9) are shown in Fig.5(c) and whose by thresholding are shown in Fig.5(d). Let us define an estimated error ϵ_k by

$$\epsilon_k = \sum_{i=0}^{I-1} \sum_{j=0}^{J-1} |g_{ijk} - \hat{g}_{ijk}| \quad (9)$$

where g_{ijk} , \hat{g}_{ijk} expresses the gray levels of original images and estimated images, respectively, and I, J are size

of images. The wormhole regions in Fig.5(c) are estimated correctly when $k = 1, 2, 3$, but have the errors such as $2[\text{pixels}]$ when $k = 4, 5$, as shown in Table 1. Those errors are caused by wormhole regions which are connected to the background. We also make the region estimation for X-ray CT images. Figure 6 shows that our method can extract wormhole regions sufficiently, connected with a background such as at slices of $k = 35, 99$ comparing with the results by thresholding. The error of $k = 35$ can be decreased by **step 2** of **Algorithm 2** (Fig.7(a)). However, the error shown in the portion surrounded with a rectangle at $k = 99$ cannot be erased (Fig.6(g), Fig.7(b)). We then need further consideration.

4.2. Experiment of graph structure extraction

For the synthetic images so that positions and forms of wormhole regions are known as shown in Fig.8(a). We make the experiment of the graph structure extraction. Figure 8(b) visualizes the wormhole regions in three dimensions. Figure 8(c) shows the result of the graph structure extraction and (d) shows restoration images $R = \{r_{ijk}\}$ of Eq.(8) from $C_{k,l}$ which are possessed by the nodes $n_{k,l}$ of the graph of (c). The nodes and edges were obtained correctly. We also achieved the same experiment to a set of X-ray CT images of Fig.9(a). There are many wormhole

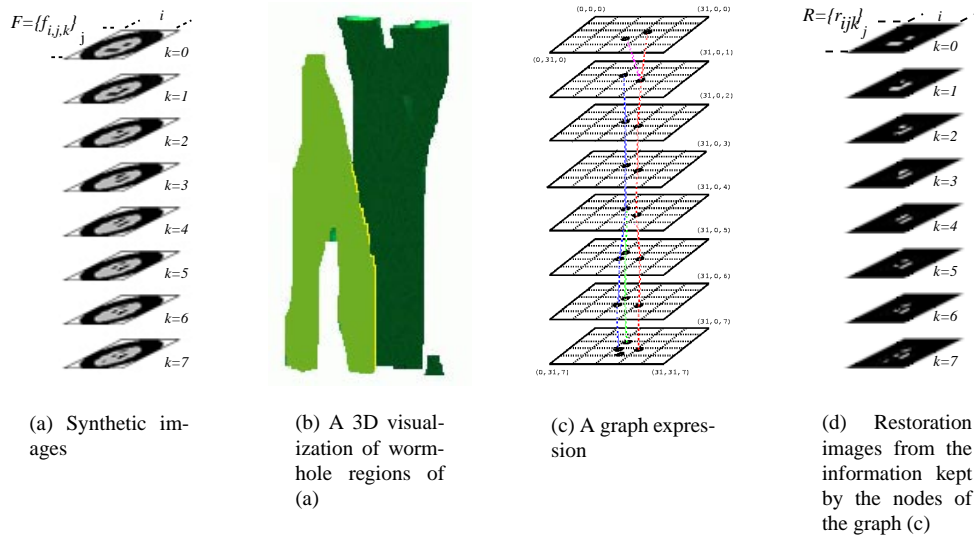


Figure 8. Graph structure extraction for test images

regions and it is hard to check the positions and the sizes of the wormholes. Figure 9(b) is the 3D visualization of wormholes, (c) shows the edges and nodes of a graph structure of (a), (d) is reconstructed wormhole images from the graph of (c). Figure 9 shows that our method extracts a graph structure correctly for a set of real X-ray CT images.

4.3. Visualization of all wormhole regions

Figure 10(a) shows wormhole regions of a wooden statue extracted by our method. The numbers in Fig.10(b) and (c) indicate the node numbers and Fig.10(d) shows the edges between the nodes. The part of Fig.10(a) is also shown in (b) and (c) from the different views, front and top. Thus, we can see the relation of wormholes from Fig.10.

The visualization will help the diagnosis of damaged statues by a sculptor. Since a sculptor can see a statue only from the exterior, the interior information such as positions, sizes and connectivity relations of wormhole regions will be useful for the diagnosis. Moreover, it is also useful for the restoration such that where and how the filler will be put.

5. Conclusions

This paper describes an image feature extraction and analysis for the restoration of damaged wooden statues by X-ray CT images. Especially, we focused on wormhole regions which are the most serious damage and extracted by using X-ray CT values. We obtain the structures of wormhole regions in two steps. First

we estimate the region of a statue including wormhole regions by the 3D figure fusion processing. Second we extract a 3D graph structure of the wormhole regions. We also visualized a graph structure for a set of X-ray CT images. Our method contributes to the restoration work.

Acknowledgments

We express our thanks to the offer and help of M.D. K. Kobayashi at Kanazawa University Hospital to provide the image data for our experiments.

References

- [1] T. Iwasaki, "Preservation and restoration of cultural asset" (in Japanese), SNHK books (1977).
- [2] J. Toriwaki, "Digital image processing for image understanding(II)" (in Japanese), SHOKODO (1988).
- [3] M. Kass, A. Witkin, D. Terzopoulos, "Snakes: Active Counter Models", Proc.1st. ICCV, pp. 259-269 (1987).
- [4] K. Mori, J. Hasegawa, J. Toriwaki, H. Anno, K. Katada, "Extraction and Visuarization of Bronchu from 3-D Images of Lung", LNCS;905 Computer Vision, Virtual Reality and Robotics in Medicine, N. Ayache(Ed.), pp. 542-548, Springer (1995).
- [5] T. Endoh, K. Mori, "Automated extraction of lung area using rib cage structure in 3-D chest X-ray CT images" (in Japanese), IEICE, D-II, Vol. J81, No. 6, pp. 1429-1438 (1998).
- [6] J. Hasagawa, K. Mori, "Automated extraction of lung cancer lesions from multi-slice chest CT images by using three-dimensional image processing" (in Japanese), IEICE, D-II, Vol. J76, No. 8, pp. 1587-1594 (1993).

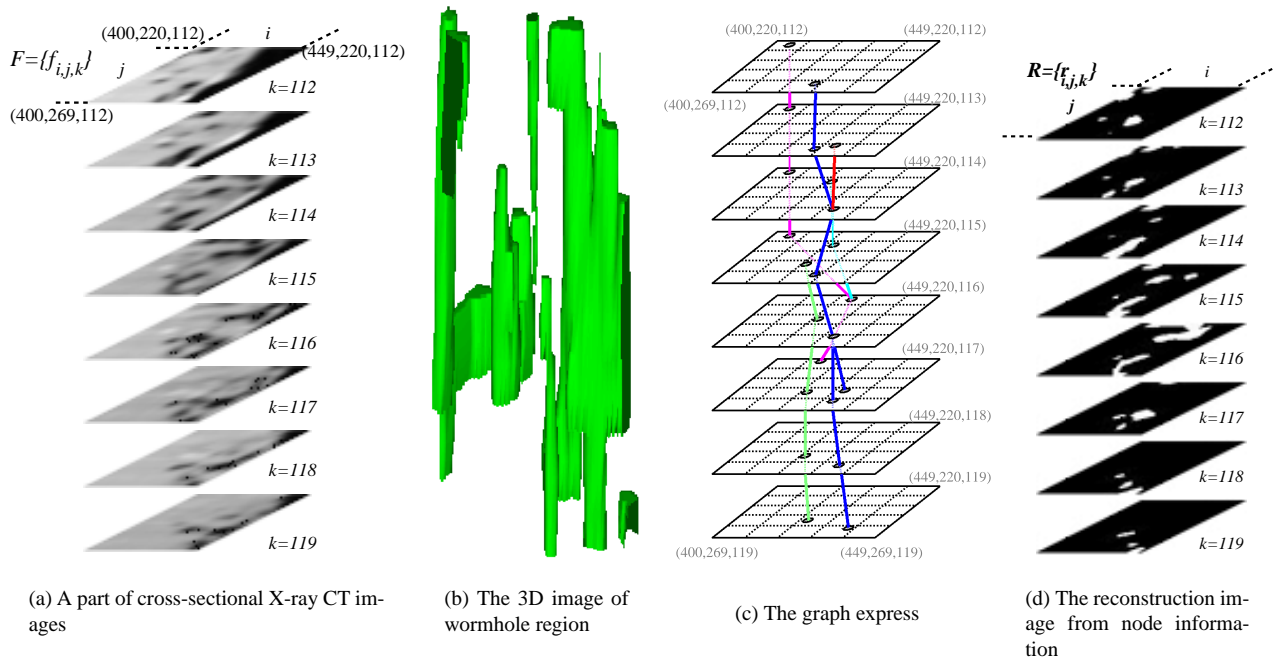


Figure 9. The result of graph structure extract

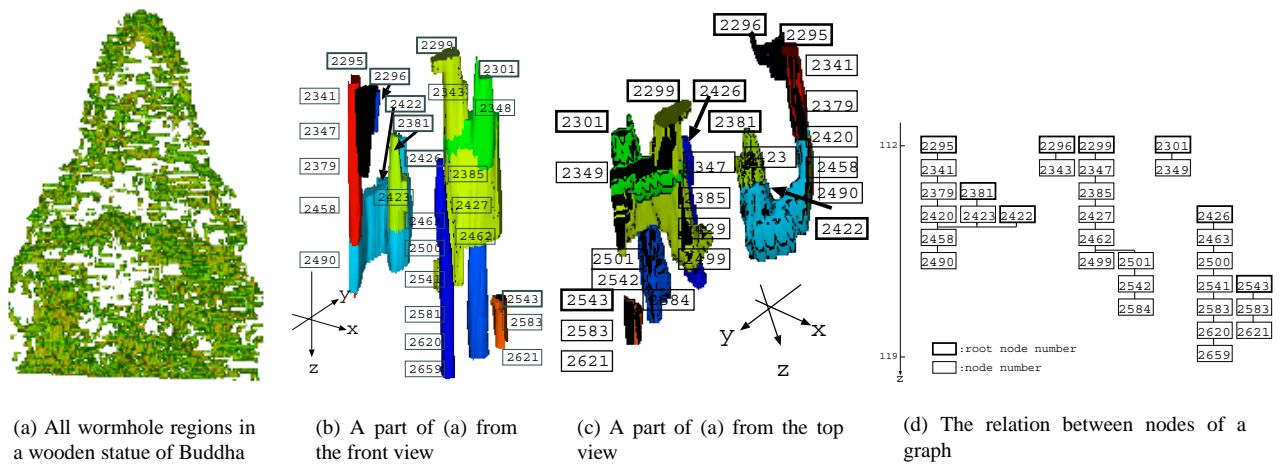


Figure 10. A graph structure of wormhole regions